Crystallization behaviors of ultrathin Al-doped HfO_2 amorphous films grown by atomic layer deposition*

Xue-Li Ma(马雪丽)[1,3], Hong Yang(杨红)[1,3], Jin-Juan Xiang(项金娟)[1,3], Xiao-Lei Wang(王晓磊)[1,3], Wen-Wu Wang(王文武)[1,3,†], Jian-Qi Zhang(张建齐)[2], Hua-Xiang Yin(殷华湘)[1,3], Hui-Long Zhu(朱慧珑)[1,3], and Chao Zhao(赵超)[1,3]

[1] *Integrated Circuit Advanced Process R & D Center, Institute of Microelectronics, Chinese Academy of Sciences, Beijing* 100029, *China*
[2] *National Center for Nanoscience and Technology, Beijing* 100190, *China*
[3] *University of Chinese Academy of Sciences, Beijing* 100049, *China*

(Received 14 October 2016; revised manuscript received 22 November 2016; published online 10 January 2017)

In this work, ultrathin pure HfO_2 and Al-doped HfO_2 films (about 4-nm thick) are prepared by atomic layer deposition and the crystallinities of these films before and after annealing at temperatures ranging from 550 °C to 750 °C are analyzed by grazing incidence x-ray diffraction. The as-deposited pure HfO_2 and Al-doped HfO_2 films are both amorphous. After 550-°C annealing, a multiphase consisting of a few orthorhombic, monoclinic and tetragonal phases can be observed in the pure HfO_2 film while the Al-doped HfO_2 film remains amorphous. After annealing at 650 °C and above, a great number of HfO_2 tetragonal phases, a high-temperature phase with higher dielectric constant, can be stabilized in the Al-doped HfO_2 film. As a result, the dielectric constant is enhanced up to about 35. The physical mechanism of the phase transition behavior is discussed from the viewpoint of thermodynamics and kinetics.

Keywords: Al-doped HfO_2 ultrathin film, phase transition, thermodynamics, kinetics

PACS: 77.55.D–, 81.40.–z, 82.60.Nh, 73.40.Qv **DOI:** 10.1088/1674-1056/26/2/027701

1. Introduction

Recently, post high-*k* gate dielectric materials with superior properties to those of the conventional high-*k* materials have been studied extensively in advanced gate-stack structures in further scaled metal-oxide–semiconductor field-effect transistor (MOSFET).[1–5] In general, the dielectric constants of high-*k* materials can be affected by their degrees of crystallinity, crystal structures, and crystallographic orientations, in addition to their stoichiometric compositions. In the case of HfO_2, it possesses four crystalline phases (monoclinic, tetragonal, cubic, and orthorhombic), and the cubic and tetragonal high-temperature hafnia phases show much higher dielectric constants (on the order of 30–40) than the monoclinic and amorphous phases.[6–8] There have been many reports showing that the dielectric constant of HfO_2 can be enhanced by doping Y_2O_3, Al_2O_3, SiO_2, etc. due to the change in the crystal structure of the film.[9–16] However, these studies have typically relied on films with thickness values larger than 10 nm, few articles have been published which strived to understand how the dielectric constant is related to the crystal structure of ultrathin (< 5 nm) HfO_2 film.

In this letter, we report an experimental result based on phase transition engineering that a great deal of tetragonal phase HfO_2 can be stabilized in the ultrathin (about 4-nm thick) HfO_2 film when being annealed at temperatures above 650 °C due to the addition of small concentration Al atoms into HfO_2 film. In addition, we study the phase transition behavior of ultrathin Al-doped HfO_2 film from the viewpoint of thermodynamics and kinetics for the first time. A model for the total Gibbs free energy is proposed to help to understand the physical mechanism behind.

2. Experiment

The pure HfO_2 and Al-doped HfO_2 films were deposited on 8-inch (1 inch = 2.54 cm) diameter p-type (100) Si substrates at 300 °C by thermal ALD. The $Hf[N(CH_3)(C_2H_5)]_4$ (TEMAH) and $Al(CH_3)_3$ (TMA) were used as the Hf and Al precursors, respectively. H_2O was used as an oxygen source. Details of the deposition processes have been published elsewhere.[17,18] The deposition rates of the ALD HfO_2 and Al_2O_3 films were respectively about 0.08 nm/cycle and 0.1 nm/cycle calibrated by x-ray reflection (XRR) and high resolution transmission electron microscopy (HRTEM). An Al–O layer was inserted into the HfO_2 film by substituting one Hf–O cycle with one Al–O cycle among total ALD cycles to incorporate the Al atoms into the HfO_2 film. Accordingly to grow the ultrathin pure HfO_2 film and Al-doped HfO_2 film with appropriate Al atom concentration, we controlled the

*Project supported by the National High Technology Research and Development Program of China (Grant No. 2015AA016501) and the National Natural Science Foundation of China (Grant Nos. 61574168 and 61504163).

†Corresponding author. E-mail: wangwenwu@ime.ac.cn

© 2017 Chinese Physical Society and IOP Publishing Ltd

number of total ALD cycles to 51 for the pure HfO_2 film, and 25c HfO_2/1c Al_2O_3/25c HfO_2 for the Al-doped HfO_2 film. Post deposition anneal (PDA) was performed at temperatures ranging from 550 °C to 750 °C for 60 s in an N_2 atmosphere. ALD TiN/W and PVD Al were deposited as the top and bottom electrode respectively followed by forming gas annealing performed at 400 °C for 20 min in a 95% N_2/5% H_2 atmosphere to form the metal-oxide-semiconductor capacitors. We used grazing incidence x-ray diffraction (GIXRD) to determine the crystallinities of these films. The capacitance–voltage (C–V) measurement was performed by using a C–V analyzer (Keithley 4200) at a frequency of 1 MHz and the equivalent oxide thickness (EOT) was calculated from the accumulation capacitance with considering the quantum effect.

3. Results and discussion

The crystallinities of the pure HfO_2 and Al-doped HfO_2 film before and after annealed at temperatures ranging from 550 °C to 750 °C are investigated by GIXRD as shown in Fig. 1. The x-ray wavelength is 0.154 nm and the x-ray beam is incident at a grazing angle of 0.2°. As shown in Fig. 1(a), which displays the GIXRD spectra in a 2θ range of 26°–39° for the pure HfO_2 films, the GIXRD pattern of as-deposited pure HfO_2 film shows no peak, reflecting its amorphous nature, while the profile of pure HfO_2 film annealed at 550 °C–750 °C shows two peaks around 28.4° and 35.4°. Figure 1(b) displays the GIXRD spectra in a 2θ range of 26°–39° for the Al-doped HfO_2 films annealed at different temperatures. The as-deposited Al-doped HfO_2 film is also amorphous. However, compared with the GIXRD pattern of the pure HfO_2 film annealed at 550 °C, the profile of Al-doped HfO_2 film annealed at 550 °C shows no peak, indicating that the incorporation of Al_2O_3 can increase the thermal stability of HfO_2 film, which has been reported in previous literature.[19–21] The profiles of Al-doped HfO_2 films annealed at 650 °C and 750 °C also show two peaks, the first peak is located around 30.4° and the second one is located around 36°. Interestingly, compared with the first peak of pure HfO_2 film, the peak value and intensity of the Al-doped HfO_2 film are obviously increased. We find that the intensity of the peak in a 2θ range of 26°–33° originates from three partial overlapped peaks with Gaussian shapes. As shown in Figs. 1(c) and 1(d), the three peaks of pure HfO_2 film are located at 27.5°, 28.4°, and 30.1° corresponding to orthorhombic phase (O), monoclinic phase (M), and tetragonal phase (T), respectively. It can be concluded that the pure HfO_2 films annealed at 650 °C and 750 °C are composed of orthorhombic, monoclinic and tetragonal phase, among which the monoclinic phase is dominant. While the three peaks of Al-doped HfO_2 film are located at 29.1°, 30.1° (T), and 31.3° (M). We think, the peak located at 29.1° is related to Hf_xAl_yO. Compared with the pure HfO_2 film, the Al-doped HfO_2 film has three peaks whose intensities are

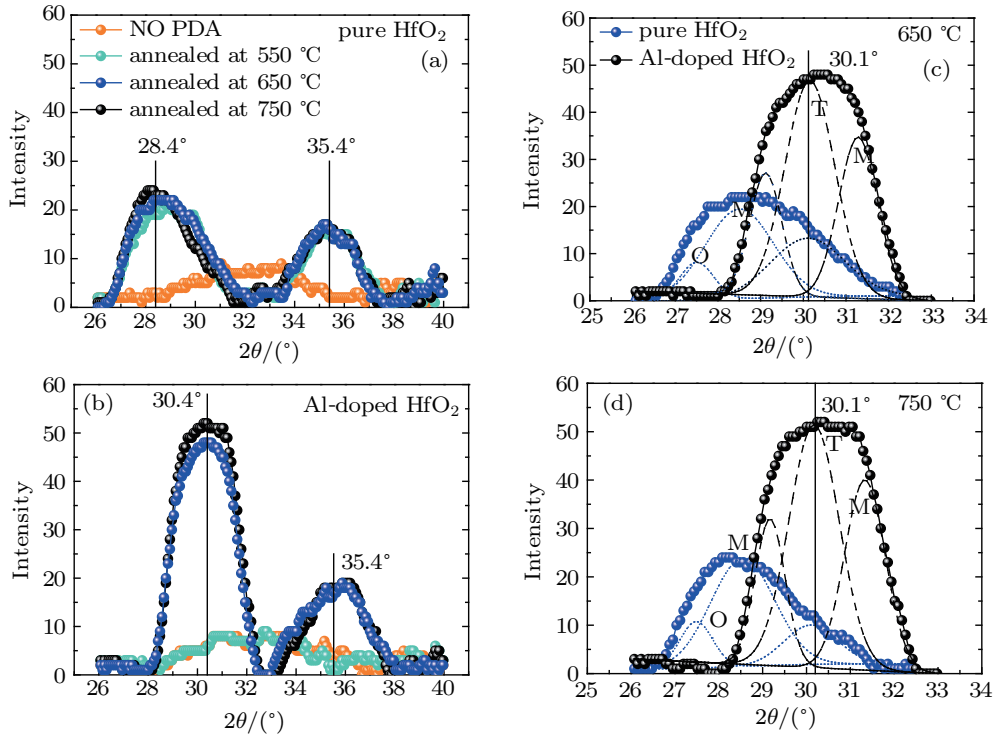


Fig. 1. (color online) GIXRD spectra of (a) pure HfO_2 films, (b) Al-doped HfO_2 films before and after annealed at temperatures ranging from 550 °C–750 °C. A superimposed view of GIXRD patterns showing the structure phase difference between pure HfO_2 film and Al-doped HfO_2 film (c) annealed at 650 °C and (d) annealed at 750 °C. The blue short dotted lines and gray short dash lines represent the fitting components of pure HfO_2 film and Al-doped HfO_2 film, respectively. The thickness of each film is fixed at 4 nm.

increased. Moreover, the strongest peak intensity is observed for the tetragonal phase, indicating that the tetragonal phase is dominant in each of the Al-doped HfO_2 films annealed at 650 °C and 750 °C, which is different from the scenarios of pure HfO_2 films. Additionally, there are only slight increases in the peak intensity for all films with the annealing temperature increasing from 650 °C to 750 °C due to the ultrathin film thickness. According to the GIXRD results, we conclude that the phase transition temperature of hafnia is reduced due to the addition of ∼4% Al atoms. Especially for the tetragonal phase, which was reported to be about 1700 °C for thick hafnia in Ref. [22]. In other words, the Gibbs energy barrier for the nucleation of crystallographic hafnia phase is reduced from the viewpoint of kinetics, and the Gibbs energy barrier for the tetragonal phase is smaller than that for the monoclinic phase. In addition, the stabilization of metastable tetragonal HfO_2 phase by adding ∼4% Al atoms indicates that the Gibbs free energy of the tetragonal HfO_2 phase is reduced approximately to the Gibbs free energy of the monoclinic HfO_2 phase from the viewpoint of thermodynamics.

The experimental MOS structure with 4-nm Al-doped HfO_2 film and terraced thickness SiO_2 film as dielectric film is shown in Fig. 2, the Al-doped HfO_2 thickness is fixed at 4 nm because the purpose of this study is to examine the ultrathin (about 4 nm) Al-doped HfO_2 film properties. Figures 3(a)–3(c) are the C-V curves of MOS capacitors with dielectric films annealed at 550 °C, 650 °C, and 750 °C, respectively. The equivalent oxide thickness (EOT) is extracted from the accumulation capacitance.

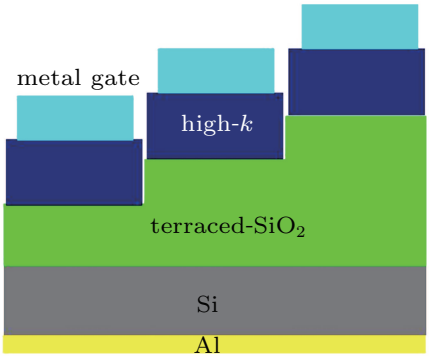


Fig. 2. (color online) Schematic diagram of experimental MOS structure.

Figures 4(a)–4(c) show the relationship plots between the SiO_2 physical thickness and the equivalent oxide thickness (EOT) of MOS capacitors with dielectric films annealed at 550 °C, 650 °C, and 750 °C, respectively. Then, the dielectric constant of each film can be determined from the intercept of its plot. Figure 4(d) clearly shows that Al-doped HfO_2 films annealed at 650 °C and 750 °C each have a significant enhancement of dielectric constant over pure HfO_2 despite the fact that Al_2O_3 has a lower permittivity (∼9) than pure HfO_2 (∼ 20). This can be attributed to the fact that a great number of tetragonal phases are formed in the film annealed at 650 °C, which has a higher dielectric constant than amorphous and monoclinic phase. When the annealing temperature reaches 750 °C, the dielectric constant increases very slowly (∼ 36) due to the limitation to the number of the tetragonal phases , which is attributed to the small Al atom concentration and ultrathin HfO_2 film thickness. The dielectric constant of the Al-doped HfO_2 film annealed at 550 °C keeps almost unchanged, which can be accounted by the fact that the film remained amorphous at 550 °C. The dielectric constant behavior is consistent with the GIXRD results discussed above.

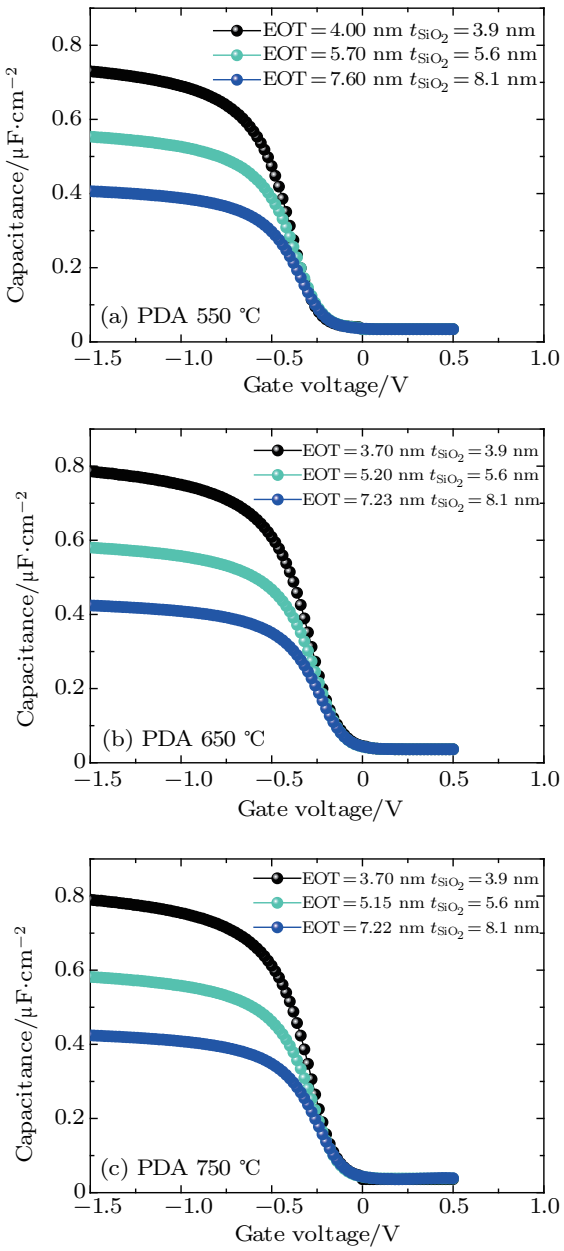


Fig. 3. (color online) The *C*–*V* curves of MOS capacitors with 4-nm Al-doped HfO_2 film and different-thickness SiO_2 films as dielectric films annealed at (a) 550 °C, (b) 650 °C, and (c) 750 °C.

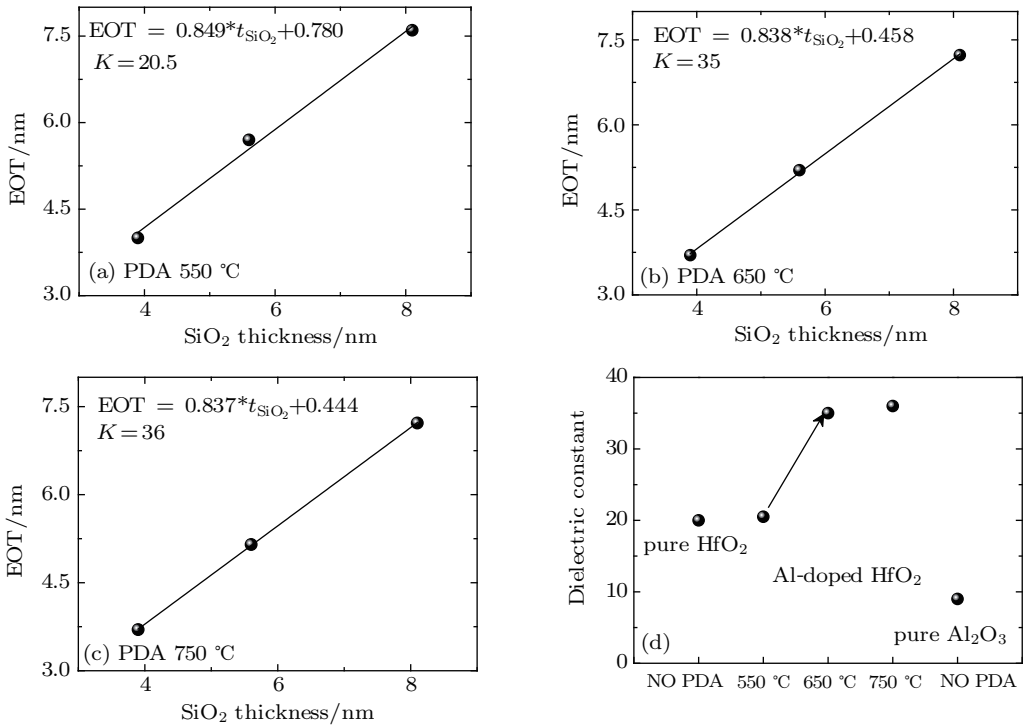


Fig. 4. Relationship plots between SiO_2 physical thickness and EOT of MOS capacitor with dielectric film annealed at (a) 550 °C, (b) 650 °C, (c) 750 °C, respectively. The dielectric constant (represented by "*K*" in the above plots) is obtained from the intercept of the corresponding plot. (d) The dielectric constants versus annealing temperature for different films.

In general, crystallization is dominated by both kinetic and thermodynamic factors. Figure 5(a) shows the Gibbs free energy schematic diagram of the phase transition of Al-doped HfO_2 film. G_m and G_t represent the Gibbs free energies of monoclinic and tetragonal phase of pure HfO_2, and G'_m and G'_t represent the Gibbs free energies of monoclinic and tetragonal phase of Al-doped HfO_2 film annealed at 650 °C, respectively. G_{a-HfO_2} and $G_{Al_2O_3}$ represent the Gibbs free energies of amorphous pure HfO_2 and Al_2O_3, and X_{HfO_2}, and $X_{Al_2O_3}$ represent the atomic mole percentages of HfO_2 and Al_2O_3 in the Al-doped HfO_2 film, about 96% and 4% respectively. G^0, the total Gibbs free energy of as-deposited Al-doped HfO_2, is approximately equal to G_{a-HfO_2} as given in Eq. (1). So $\Delta G'_{a-m} = G'_m - G_{a-HfO_2} < 0$ and $\Delta G'_{a-t} = G'_t - G_{a-HfO_2} < 0$ can be taken as the thermodynamic driving force for the phase transition of Al-doped HfO_2 from amorphous to crystallization. On the way of transiting HfO_2 phase from amorphous to either monoclinic or tetragonal phase, the system need to overcome the Gibbs energy barrier by thermal activation. G^*_m and G^*_t represent the Gibbs energy barriers for the nucleation of pure HfO_2 from amorphous to monoclinic and tetragonal phase respectively. ΔG^*_m and ΔG^*_t represent the decreases of the Gibbs energy barrier for the nucleation of Al-doped HfO_2 from amorphous to monoclinic and tetragonal phase respectively.[23,24] Figure 5(b) describes the variations of the Gibbs free energy of a growing spherical new phase particle with particle radius r. If a particle with $r = r_{crit}$ occurs, the system can lower its Gibbs energy spontaneously with the new phase particle growing. Considering the formation of a spherical new phase (monoclinic or tetragonal) particle of radius r in amorphous pure HfO_2 film, the total Gibbs energy change ΔG can be given as Eq. (2). $\Delta G_{chem} \sim r^3 (< 0)$ is the change in chemical energy driving the transformation. $\Delta G_{int} \sim r^2 (> 0)$ is the change in interface energy associated with the occurrence of interface between new phase and parent phase opposing the transformation. $\Delta G_{str} \sim r^3 (> 0)$ is the change in strain energy associated with the volume expansion opposing the transformation.[23] Similarly, the total Gibbs energy change $\Delta G'$ of Al-doped HfO_2 film can be given as Eq. (3). Compared with Eq. (2), equation (3) has the fourth term $\Delta G_{Al-induced} (< 0)$. After 550-°C annealing, Al atoms remain in Al_2O_3 layer because there is no enough thermal energy to break down Al–O bond, and the incorporation of Al_2O_3 can increase the thermal stability of HfO_2 film as reported before. After 650-°C annealing, Al atoms will diffuse from Al_2O_3 layer into HfO_2 layer and substitute Hf atoms thus causing additional strain energy $\Delta G_{Al-induced}$ associated with the local lattice distortion. As the result of thermal fluctuation and by chance, a local atomic rearrangement will occur such that a new phase particle is created compatible to the thermodynamically preferred phase. The formation of new phase around Al atoms can gradually re-

lease part of the strain energy with the particle growing. It follows from Fig. 5(b) that $\Delta G_{\mathrm{Al-induced}}$ can result in a decrease in the nucleation barrier G^* for either monoclinic or tetragonal phase HfO_2. On the other hand, for alumina, the Al coordination number has a value between 4 and 6, and the Al–O bond lengths are between 1.71 Å and 1.79 Å.[25] For monoclinic phase HfO_2, the Hf coordination number is seven and the average Hf–O_I and Hf–O_{II} bond lengths are 2.086 Å and 2.197 Å, respectively.[26] For tetragonal phase HfO_2, the Hf coordination number is eight and the Hf–O bond lengths are equally distributed at 2.07 Å and 2.37 Å.[27] Obviously, there are four shorter Hf–O bonds in tetragonal phase HfO_2 that will facilitate the formation of Al–O bonds with relatively small lattice distortion. In other words, the absolute value of $\Delta G_{\mathrm{Al-induced}}$ for tetragonal phase HfO_2 is larger than that for monoclinic phase HfO_2. Therefore, the change of the Gibbs free energy of tetragonal phase for Al-doped HfO_2 is larger than that for monoclinic phase and the energy difference between the two phases is reduced. Theoretical study by using the first-principles calculations of doped HfO_2 has also indicated a similar conclusion.[27,28] Moreover, the decrease in the nucleation barrier for tetragonal phase HfO_2 ΔG_{t}^* is larger than that for monoclinic phase HfO_2 ΔG_{m}^*. Hence, 650-°C annealing can supply enough thermal agitation to rearrange the involved Hf atoms and O atoms to form a tetragonal phase nucleus. As can be seen in our GIXRD result, a multiphase consisting of monoclinic phase and tetragonal phase is formed in the Al-doped HfO_2 film when being annealed at temperatures above 650 °C and the tetragonal phase is dominant. G^0, ΔG, and $\Delta G'$ are expressed as

$$\begin{aligned} G^0 &= X_{\mathrm{HfO_2}} * G_{\mathrm{a-HfO_2}} + X_{\mathrm{Al_2}O_3} * G_{\mathrm{Al_2O_3}} \\ &= G_{\mathrm{a-HfO_2}} + \left(G_{\mathrm{Al_2O_3}} - G_{\mathrm{a-HfO_2}}\right) * X_{\mathrm{Al_2O_3}}, \quad (1) \\ \Delta G &= \Delta G_{\mathrm{chem}} + \Delta G_{\mathrm{int}} + \Delta G_{\mathrm{str}}, \quad (2) \\ \Delta G' &= \Delta G_{\mathrm{chem}} + \Delta G_{\mathrm{int}} + \Delta G_{\mathrm{str}} + \Delta G_{\mathrm{Al-induced}}. \quad (3) \end{aligned}$$

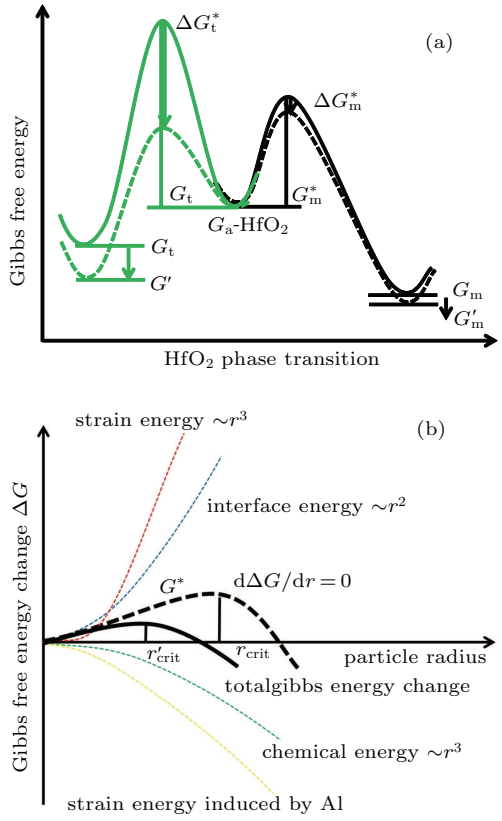


Fig. 5. (color online) (a) Gibbs free energy schematic diagram of phase transition of Al-doped HfO_2 film from amorphous to crystallization. (b) Variations of Gibbs free energy of a growing spherical new phase particle with particle radius r.

4. Conclusions

In this work, the dielectric constant of ultrathin HfO_2 film is enhanced to ~ 35 through phase transition by adding $\sim 4\%$ Al atoms and annealing at 650 °C. The higher dielectric constant is due to the stabilization of a great number of HfO_2 tetragonal phases in the Al-doped HfO_2 film. This behavior is discussed from the viewpoint of kinetics that the Gibbs energy barrier for the tetragonal phase is smaller than that for the monoclinic phase in the case of Al-doped HfO_2 film. In addition, the stabilization of metastable tetragonal phase HfO_2 by adding $\sim 4\%$ Al atoms indicates that the Gibbs free energy of the tetragonal phase HfO_2 is reduced approximately to the Gibbs free energy of the monoclinic phase HfO_2 from the viewpoint of thermodynamics. Thus, the 4%-Al-doped HfO_2 film annealed at 650 °C can be a promising candidate for the advanced gate-stack structures in further scaled MOSFET.

References

[1] Chen Y H, Chen C Y, Cho C L, Hsieh C H, Wu Y C, Chang-Liao K S and and Wu Y H 2015 *Proceedings of IEDM Tech. Dig.*, December 7–9, 2015, Washington, D.C., USA, p. 576
[2] Wu C Y, Hsieh C H, Lee C W and Wu Y H 2015 *Appl. Phys. Lett.* **106** 053508
[3] Cisneros-Morales M C and Aita C R 2011 *Appl. Phys. Lett.* **98** 051909
[4] Fu C H, Chang-Liao K S, Li C C, Ye Z H, Hsu F M, Wang T K, Lee Y J and Tsai M J 2012 *Appl. Phys. Lett.* **101** 032105
[5] Bethge O, Abermann S, Henkel C and Bertagnolli E 2009 *Thin Solid Films* **517** 5543
[6] Choi J H, Mao Y and Chang J P 2011 *Mater. Sci. Eng. R* **72** 97
[7] Robertson J 2008 *J. Appl. Phys.* **104** 124111
[8] Zhao X Y and Vanderbilt D 2002 *Phys. Rev. B* **65** 233106
[9] Tomida K, Kita K and Toriumi A 2006 *Appl. Phys. Lett.* **89** 142902
[10] Kita K, Kyuno K and Toriumi A 2005 *Appl. Phys. Lett.* **86** 102906
[11] Park T J, Kim J H, Jang J H, Lee C K, Na K D, Lee S Y, Jung H S, Kim M, Han S and Hwang C S 2010 *Chem. Mater.* **22** 4175
[12] Park P K and Kang S W 2006 *Appl. Phys. Lett.* **89** 192905
[13] Ragnarsson L A, Adelmann C, Higuchi Y, Opsomer K, Veloso A, Chew S A, Röhr E, Vecchio E, Shi X P, Devriendt K, Sebaai F, Kauerauf T, Pawlak M A, Schram T, Elshocht S V, Horiguchi N and Thean A 2012 *Proceedings of VLSI Tech. Dig.*, June 12–15, 2012, Honolulu, USA, p. 27
[14] Adelmann C, Schram T, Chew S A, Woicik J C, Brizzi S, Tallarida M, Schmeisser D, Horiguchi N, Elshocht S V and Ragnarsson L A 2014 *Appl. Phys. Lett.* **104** 122906
[15] Yang Y, Zhu W J, Ma T P and Stemmer S 2004 *J. Appl. Phys.* **95** 3772

[16] Govindarajan S, Böscke T S, Sivasubramani P, Kirsch P D, Lee B H, Tseng H H, Jammy R, Schröder U, Ramanathan S and Gnade B E 2007 *Appl. Phys. Lett.* **91** 062906
[17] Hackley J C, Gougousi T and Demaree J D 2007 *J. Appl. Phys.* **102** 034101
[18] Kim H, Lee H B R and Maeng W J 2009 *Thin Solid Films* **517** 2563
[19] Yu H Y, Li M F and Kwong D L 2004 *Thin Solid Films* **462–463** 110
[20] Zhu W, Ma T P, Tamagawa T, Di Y, Kim J, Carruthers R, Gibson M and Furukawa T 2001 *Proceedings of IEDM Tech. Dig.*, December 2–5, 2001, Washington, D.C., USA, p. 20.4.1
[21] Wilk G D, Wallace R M and Anthony J M 2001 *J. Appl. Phys.* **89** 5243
[22] STACY D W and WILDER D R 1975 *J. Am. Ceram. Soc.* **58** 285
[23] Mittemeijer E J 2011 *Fundamentals of Materials Science* (Berlin/Heidelberg: Springer-Verlag) pp. 371–380
[24] Gottstein G 2004 *Physical Foundations of Materials Science* (Berlin/Heidelberg: Springer-Verlag) pp. 389–422
[25] Gutiérrez G and Johansson B 2002 *Phys. Rev. B* **65** 104202
[26] Wang J and Li H P and Stevens R 1992 *J. Mater. Sci.* **27** 5397
[27] Lee C K, Cho E, Lee H S, Hwang C S and Han S 2008 *Phys. Rev. B* **78** 012102
[28] Saitoh M, Mizoguchi T, Tohei T and Ikuhara Y 2012 *J. Appl. Phys.* **112** 084514